Speed Control of Hydraulic Motor System with Swashplate DC-Controlled Pump

Dr. Amjed J. Humaidi* & **Dr. Majid A. Oleiwi***

Received on:8/10/2008
Accepted on:4/6/2009

Abstract

In a previous study, speed-controlled hydraulic motor system has employed a DC motor for changing the swashplate angle of a variable displacement piston pump. However, the speed control has been performed by a flow modulation valve which is permitted to bypassing the flow of the hydraulic motor when the speed exceeds the set value. In the present work, another speed control configuration has been proposed with the pump and hydraulic motor are permitted to perform reversal actions. The conventional proportional, integral and derivative (PID) controller has been introduced to manipulate the speed error such that it could achieve the required performance. The specification required by the PID controller is to reach the command speed as fast as possible with minimum peak overshoot. Also, the effectiveness of the suggested controller against changing of system parameters is considered. The modeling of the speed control system components is detailedly presented, including the dynamic of swashplate, and one can easily see that the system is of a nonlinear nature. The state space representation of the complete system has been developed and the program codes are listed inside an m-file, which is instantaneously called by an s-function within SIMULINK library.

Keywords: Variable displacement piston pump, hydraulic motor, PID controller, Matlab/Simulink/s-function.

السيطرة على سرعة المنظومة الهايدروليكية بمضخة ذات ازاحة متغيرة ومسيطر عليها باستخدام محرك تيار مستمر

الخلاصة

في دراسة سابقة، تمت السيطرة على سرعة المحرك الهايدروليكي وذلك باستخدام محرك تيار مستمر للسيطرة يقوم بتغير زاوية (swashplate). مع ذلك، فان سرعة المحرك يتم تغيرها باستخدام صمام تغير الجريان (valve flow modulation) الذي يوفر مسلك اخر لجريان السائل الى المحرك الهايدروليكي وبدوره يؤدي الى تقليل معدل الجريان الى المحرك الهايدروليكي عندما تتجاوز سرعته السرعة المطلوبة.

في هذه الدراسة، تم اقتراح صيغة اخرى للسيطرة على سرعة المحرك الهايدروليكي بحيث يمكن للمحرك تغير اتجاه سرعته وذلك بتغير اتجاه الجريان في المضخة الهايدروليكية. وتم استخدام المسيطر التناسبي التكاملي لغرض معالجة الخطأ في قيمة السرعة لتحقيق الاداء المطلوب، والذي يتمثل بالحصول على اسرع استجابة باقل قمة (peak overshoot).

* Control and System Engineering Department, University of Technology/Baghdad

تم تناول نمذجة العناصر المكونة لمنظومة السيطرة المغلقة، متظمنا" الحركة الداينامكية لـــ (swashplate)، حيث يمكن ملاحظة الطبيعة اللاخطية لمنظومة السيطرة، وكذلك تم تمثيل فضاء المتغيرات (state space) للمنظومة الكامـــلة، وعـــرض البرنـــامج وتنفيذه باستخـــدام (Matlab/Simulink/s-function).

Nomenclature

D_m : Volumetric displacement of the motor.
J_m : Inertia of the motor and the load.
C_{tm} : Motor leakage coefficient.
B_m : Motor damping ratio.
T_{fm} : Motor coulomb friction torque.
V_m : Volume of the motor and pipe.
K_t : Torque sensitivity.
K_b :Back EMF constant of DC motor.
J_d : Moment of Inertia of the motor rotor.
B_d : Viscosity damping coefficient.
w_{rp} : Rotational speed of pump prime mover.
N : Number of pistons.
A_p : Piston area.
B_{sw} : Viscous damping ratio of the swashplate.
R_p : Piston pitch radius.
D_p : Maximum pump displacement.
b_e : Bulk modulus of the fluid.
C_{tp} : Total pump leakage flow coefficient.
V_p : Volume of pump (high pressure side).
J_{sw} : Average swashplate yoke inertia
S_1 : Simplified pump model constant.
S_2 : Simplified pump model constant.
T_f : Torque due to friction losses.
T_p : Torque relating to pressure effect.
T_r : Torque caused by barrel rotation.
T_{ds} :Static friction torque of DC motor
T_{dc} : Coulomb friction torque of DC motor.
B_d : Viscous damping.
E : The input voltage of DC motor
e_b : Back EMF voltage.
i : The armature current of DC motor.
R : The terminal resistance of the DC motor windings
L : The terminal inductance of the DC motor windings
q_{sw} :The angular position of the motor shaft and pump swashplate.
T_d : The torque developed at the shaft of the motor
w_{sw} : The angular velocity of the swashplate.
T_{sw} : The load exerted by the swashpate.
$K_{p1,2}$: Pressure torque constants.
Q_{pidea} : The ideal flow rate of the pump.
Q_p : Output flow of the pump.
Q_{ip} :Internal leakage flow of the pump.
Q_{ep} : External leakage flow of the

pump

V : Volume of the pump forward chamber.

C_{tp} : Total leakage flow coefficient of the pump.

C_{im} : Internal leakage coefficient of the hydraulic motor.

C_{em} : External leakage coefficient of the hydraulic motor

D_p : Displacement of the pump.

D_m : Volumetric displacement of the hydraulic motor .

q_m : Angular position of the hydraulic motor shaft.

V_m : Forward chamber volume of the hydraulic motor

Q_m : Input flow rate of the hydraulic motor.

P_m : Outlet pressure of the hydraulic motor.

K_p : Pump flow rate coefficient,

C_t : Total leakage coefficient of the pump and motor.

C_{lp} : Leakage coefficient of the pump.

C_{lm} :Leakage coefficient of the motor.

$\boldsymbol{x}$: The state vector.

$\boldsymbol{A}$: The state matrix.

$\boldsymbol{B}$: The input vector.

$\boldsymbol{u}$: The input of the dc-motor.

$\boldsymbol{B_T}$: The input matrix due to torque.

$\boldsymbol{u_T}$: The torque input vector.

1. Introduction

Hydraulic drives have many advantages over other technologies. The ratio of weight, volume and inertia to available power is significantly lower than in electromechanical drives, especially for linear motion. The dynamic performance is superior when compared to electrical or electrical-mechanical drive systems in large power drive systems those systems that require an output power larger than 10 kW and a fast response speed, hydraulic drive systems are often the appropriate choice. However, compared with other systems (e.g., mechanical electrical system), hydraulic systems can be energy inefficient [1].

However, variable-displacement pumps are capable of changing the amount of flow that is delivered to the hydraulic circuit by changing the angle of the swashplate. Sensing the immediate needs of the hydraulic circuit, the discharge flow of the pump may be intelligently varied to deliver only the amount of flow that is required by the system at any given instant in time. This flow-varying feature of the variable-displacement pump has increased the efficiency of hydraulic circuitry [2].

Within the past fifteen years, a significant amount of attention has been directed toward the control issues of variable-displacement axial-piston pumps. One of the interesting studies has been done by Tonglin [1]. The proposed hydraulic circuit was rotational speed control system as shown in Fig.(1). It mainly consisted of a variable displacement axial piston pump, a fixed displacement motor, a flow modulation valve and a relief valve.

Unlike traditional variable displacement, axial piston pumps, the

angle of the swashplate was controlled by a DC motor whose output shaft was directly attached to the swashplate through a pintle. The flow modulation valve, which functioned as a bypass flow modulation valve, was used to remove or minimize the overshoot of the hydraulic motor rotational speed after the transient. The bypass modulation valve was opened only during the overshoot and was closed under the steady state conditions.

The operation of the complete system is as follows. First, the desired rotational speed of the hydraulic motor is converted to the pump swashplate angle. Then, the DC motor drives the pump swashplate to achieve this desired angle in the shortest time possible. Accordingly, the pump supplies the appropriate flow rate to drive the hydraulic motor. During the whole operation, the bypass flow control system monitors the rotational speed of the hydraulic motor and takes an appropriate control action when the motor rotational speed exceeds the desired rotational speed. Finally, because of the improved dynamic response of the DC motor controlled pump, the desired rotational speed of the hydraulic motor should be achieved with an improved dynamic response as well; the performance of the hydraulic motor would be further improved with a reduction in the overshoot due to the bypass valve.

One important point, which one might argue from the above study, is that the study has not permitted the hydraulic motor to rotate in the reversal direction and, also, not allowed the pump to change its direction of flow. The reduction of motor speed beyond the set value is performed by the bypass valve which only acts as hydraulic motor flow reducer. Therefore, the dynamic performance crucially depends on the bypass valve, which, of course, requires a precise design and setting. Therefore, one can say that the overall system is not a closed loop system since the motor rotational speed signal is not directly fed back to the main input of the system.

In the present study, both the hydraulic motor and pump are allowed to perform the reversal actions. The bidirectional flow of the pump is satisfied by allowing the swashplate angle to reverse its direction.

The physical model of the control system considered for this study is illustrated in Fig.(2). As shown in the figure the bypass valve has been eliminated and the motor speed is measured, using a velocity sensor, and fed back to the speed set value. Therefore, two loops can be detected in the control system of Fig.(2). The outer loop which is responsible for controlling the speed of hydraulic motor and the inner loop is required to control the dynamic of the swashplate angle.

If the motor speed is deviated from the command value, an error signal will be generated and fed to the speed controller. According to the sign and value of the error, the DC motor will stern the swashplate angle such that the pump flow and then the

hydraulic motor would eliminate the generated error.

2. Mathematical Model of the System

One way to understand the system is to separate it into components for the purpose of modeling. Using a fundamental knowledge of physics, for instance the moment equilibrium and continuity equation, a model that represents the dynamics behavior of each component can be derived at the component levels. Having understood each individual component, one can understand the overall system by interconnecting the components together to obtain an overall system model [3].

2.1. Mathematical Model of the DC Motor

A permanent magnet DC motor converts electrical energy into mechanical energy by the interaction of two magnetic fields. A permanent magnet assembly produces one field; an electrical current flowing in the motor windings produces the other field. These two fields produce a torque that tends to rotate the rotor. As the rotor turns, the current in the windings is commutated to produce a continuous torque output. For a brushless DC motor, the permanent magnet is on the rotor; the windings of the DC motor are on the stator [4].

The mathematic model of a DC motor can be derived using a schematic diagram of the motor circuit shown in Figure (3).

The DC motor is assumed to consist of armature inertia J_d $(N \cdot m s^2/rad)$ with friction torque. The friction torque of the DC motor includes static friction torque T_{ds} $(N \cdot m)$, coulomb friction torque T_{dc} $(N \cdot m)$ and viscous damping B_d $(N\,m.s/rad)$.

The electrical circuit of the motor can be simply described by [4,1]

$$E = e_b + Ri + L\frac{di}{dt} \qquad \ldots (1)$$

$$e_b = K_b \dot{q}_{sw} \qquad \ldots\ldots(2)$$

where, E is the input voltage (V), e_b is back EMF voltage (V), i is the armature current (A), R is the terminal resistance of the DC motor windings (Ω), L is the terminal inductance of the DC motor windings (H), K_b is the back EMF constant of the motor $(V \cdot s/rad)$ and q_{sw} is the angular position of the motor shaft and pump swashplate (rad).

The torque developed at the shaft of the motor is proportional to the armature current (with fixed field current) and given by

$$T_d = K_t\, i \qquad \ldots\ldots(3)$$

where, K_t is the motor torque sensitivity $(N \cdot m/A)$.

The torque developed by the current in motor windings not only overcomes the friction in the DC motor and the load torque T_{sw} $(N \cdot m)$, due to swashplate assembly on the motor shaft but also accelerates the rotor.

$$T_d = J_d \ddot{q}_{sw} + B_d \dot{q}_{sw} + \frac{\dot{q}_{sw}}{\left|\dot{q}_{sw}\right|}\left(T_{ds} + T_{dc}\right) + T_{sw} \qquad \ldots(4)$$

or

$$T_d = J_d \dot{w}_{sw} + B_d w_{sw} + sgn(w_{sw})(T_{ds} + T_{dc}) + T_{sw} \quad ....(5)$$

where $w_{sw} = \dot{q}_{sw}$ is the angular velocity of the swashplate. sgn (ω_{sw}) is a signum function which accounts for static and coulomb frictions dependency on speed direction and it can be described as,

$$sgn\ (w_{sw}) = \begin{cases} 1 & w_{sw} > 0 \\ -1 & w_{sw} < 0 \end{cases} \quad ....(6)$$

2.2 Mathematical Model of the Pump

The pump model could be divided into two parts: the torque model and fluid flow model. The motion of the swashplate was described by the torque model; and the flow rate of the pump was described by the flow model.

2.2.1. Torque Model of Swashplate

The motion of the swashplate is dictated by the summation of torques acting on the swashplate and yoke assembly. Figure (4) illustrates the components and forces that have an effect on the total torque. They are [1,5]:

- The drive force applied by the DC motor,
- Pressure forces acting on the pistons,
- Inertia effects of pistons and swashplate yoke assembly,
- Forces applied by the shoe plate
- Friction and viscous damping forces acting on the yoke.

The friction and pressure are the dominant components of the net torque. The yoke rotates within the pump case which is filled with hydraulic fluid. The viscous damping torque acts on the yoke in a direction opposite to the motion of the swashplate. This is a consequence of fluid motion between the yoke and pump case. The yoke also "rubs" the inside parts of the pump through the pintle and swashplate, causing a resisting stiction.

However, if the pump is in operation, piston induced vibration inside the pump tends to eliminate stiction and hence can be assumed to be negligible [5].

The load exerted by the swashplate T_{sw} can be divided into the following torques [1,5]:

- Torque due to friction losses T_f $(N \cdot m)$
- Torque relating to pressure effect T_p $(N \cdot m)$
- Torque caused by barrel rotation T_r $(N \cdot m)$
- Torque required to overcome the swashplate inertia $J_{sw}\dot{w}_{sw}$ $(N \cdot m)$

Therefore, the torque equation of the swashplate can be given as:

$$T_{sw} = J_{sw}\dot{w}_{sw} + T_f - T_p - T_r \quad (7)$$

where J_{sw} is the average moment of inertia of swashplate yoke assembly.

The friction torque T_f includes coulomb friction T_{swc}, viscous damping friction $(B_{sw} w_{sw})$ and stiction. Since the stiction friction has been assumed negligible, the frictional torque can be represented as in reference [1,5]

$$T_f = \text{sgn}(w_{sw}) T_{swc} + B_{sw} w_{sw} \quad ....(8)$$

However, the torque applied to the swashplate due to the pressure effect

is significant. This torque is a function of both the pump pressure and swashplate angle and can be written as [1,5]

$$T_p = K_{p1} P_p - K_{p2} P_p q_{sw} \qquad (9)$$

where P_p is pump pressure (Pa), K_{p1} is pressure torque constant ($N.m/Pa$) and K_{p2} is the pressure torque constant ($N \cdot m/Pa \cdot rad$).

When the pump is in operation, there is a torque applied to the swashplate by the piston slippers. This force is a result of the inertia of pistons and the shoe plate and is known to be a function of the swashplate angle. Therefore, this torque is related to the rotation of the barrel and can be represented as

$$T_r = -S_1 - S_2 q_{sw} \qquad (10)$$

where

S_1 : Simplified pump model constant ($N \cdot m$).

S_2 : Simplified pump model constant ($N \cdot m/rad$).

Substituting Eq.s (8)-(10) into Eq.(7), one can obtain the following torque model of the swashplate:

$$T_{sw} = J_{sw} \dot{w}_{sw} + \mathrm{sgn}(w_{sw}) T_{swc} + B_{sw} w_{sw} - K_{p1} P_p + K_{p2} P_p q_{sw} + S_1 + S_2 q_{sw} \qquad ....(11)$$

Again, substitution the last equation into Eq.(5) will yield

$$T_d = J_d \dot{w}_{sw} + B_d w_{sw} + \mathrm{sgn}(w_{sw})(T_{ds} + T_{dc}) + J_{sw} \dot{w}_{sw} + \mathrm{sgn}(w_{sw}) T_{swc} + B_{sw} w_{sw} - K_{p1} P_p + K_{p2} P_p q_{sw} + S_1 + S_2 q_{sw} \qquad ....(12)$$

or

$$T_d = (J_d + J_{sw}) \dot{w}_{sw} + (B_d + B_{sw}) w_{sw} + S_1 + (S_2 + K_{p2} P_p) q_{sw} - K_{p1} P_p + a_{sw} (T_{ds} + T_{dc} + T_{swc}) \qquad (13)$$

where $a_{sw} = \mathrm{sgn}(w_{sw})$.

2.2.2 Flow Model of the Pump

The displacement of the pump is defined as follows [1,6]:

$$D_p = N A_p R_p \tan q_{sw} / p \qquad \ldots(14)$$

Where

D_p =Displacement of the pump $\left(\frac{m^3}{rad}\right)$.

R_p = Radius of the piston pitch (m),

N = Number of pistons,

A_p = Area of the piston (m^2).

Assuming that the rotational speed of the prime mover is w_{rp}, the ideal flow rate of the pump is as follows:

$$Q_{pidea} = w_{rp} D_p = \frac{w_{rp} N A_p R_p \tan(q_{sw})}{p} \qquad ..... (15)$$

The actual flow rate of the pump is less than the ideal flow rate due to the fluid leakage and fluid compression. There are two types of leakage flows in the pump. One is the internal leakage flow between the suction port and the discharge port of the pump and the other is the external leakage from the high-pressure chamber to the case drain through the pump casing. From the continuity equation, the flow equation for the pump can be written as in references [1,6,7]

$$Q_{pidea} - Q_{ip} - Q_{ep} - Q_p = \frac{V_p}{b} \dot{P}_p \qquad ...(16)$$

where

Q_p =Output flow of the pump (m^3/s)

Q_{ip} =Internal leakage flow of the pump,

Q_{ep} =External leakage flow of the pump

V =Volume of the pump forward chamber

If the suction pressure is assumed to be zero, the leakage flow of the pump (including the internal leakage and the external leakage flow) can be approximated by

$$Q_{lp} = Q_{ip} + Q_{ep} = C_{tp}\ P_p \qquad ....(17)$$

where C_{tp} ($m^3 / s \cdot Pa$) is the total leakage flow coefficient.

Substituting Eq.(15) and (17) into Eq.(16) one can get the flow model of the pump,

$$\frac{V_p}{b_e}\dot{P}_p = w_{rp}\, N\, A_p\, R_p \tan(q_{sw})/p \ - C_{tp}\ P_p - Q_p \qquad ....(18)$$

2.3. Mathematical Model of Hydraulic Motor

The motor is in this study had a stationary swashplate which was used to move the piston forward and backwards. To simplify the illustration, Fig.(5) shows the motor with only two pistons. The leakages and friction losses were lumped at these pistons.

The mathematic model of the hydraulic motor was quite similar to that of the pump. It was described by two equations: the first was the continuity equation that described flow through the motor, and the second, the torque equation that related the fluid pressure to the output motor torque.

According to the continuity equation, the flow equation is described as in reference [7]

$$\frac{V_m}{b_e}\dot{P}_p = Q_m - C_{im}(P_p - P_m) - C_{em}\, P_p - D_m \dot{q}_m \qquad ...(19)$$

Where

C_{im} = Internal leakage coefficient of the hydraulic motor ($m^3 \cdot Pa/s$),

C_{em} =External leakage coefficient of the hydraulic motor ($m^3 \cdot Pa/s$),

D_m =Volumetric displacement of the hydraulic motor (m^3/rad),

q_m =Angular position of the hydraulic motor shaft (rad),

V_m = Forward chamber volume of the hydraulic motor (m^3),

Q_m =Input flow rate of the hydraulic motor.

P_m =Outlet pressure of the hydraulic motor.

The flow rate across the hydraulic motor is affected by leakage and fluid compression. The leakage term in Eq.(19) is proportional to the pressure drop across the leakage path. Leakage in the hydraulic motor is also known to be the function of motor rotational speed but for this model, the simplified model of leakage in Eq.(19) was used. For the feasibility study, the effects of the lines between the pump and motor are considered negligible. Compressibility effects due to the volume of fluid in the

connecting lines are simply lumped into the volume of motor piston chambers.

Using Newton's second law, the torque equation of the motor is [1,7]:

$$(P_p - P_m)D_m = J_m \dot{q}_m + B_m \dot{q}_m + sgn(\dot{q}_m)T_{mc} + T_L \qquad (20)$$

where J_m is the total inertia of the hydraulic motor, B_m is the total viscous damping coefficient, T_{mc} is coulomb friction torque of the hydraulic motor, T_L is the load applied on the hydraulic motor shaft and q_m is the hydraulic angular position.

Letting $w_m = d\,q_m/dt$, Eq.(20) can be written as

$$(P_p - P_m)\,D_m = J_m \dot{w}_m + B_m w_m + a_m T_{mc} + T_L \qquad (21)$$

where

$$a_m = sgn\,(w_m) = \begin{cases} 1 & w_m > 0 \\ -1 & w_m < 0 \end{cases}$$

Since the motor outlet is usually connected to tank, then outlet pressure can be considered equal to zero ($P_m = 0$). Therefore, Eq.(19) and (21) are simplified to the following equations:

$$Q_m - C_{tm}\,P_p - D_m\,w_m = \frac{V_m}{b_e}\dot{P}_p \quad ..(22)$$

$$P_p\,D_m = J_m\,\dot{w}_m + B_m\,w_m + a_m\,T_{mc} + T_L \quad ..(23)$$

where C_{tm} is the total leakage coefficient of the motor.

If the flow from the pump Q_p is equal the value of flow into the motor Q_m, i.e,

$$Q_p = Q_m \quad ..(24)$$

then from Eq.(18), (22) and (24) one can obtain

$$K_p\,tan\,(q_{sw}) = D_m\,w_m + C_t\,P_p + \frac{V_t}{b_e}\dot{P}_p \qquad (25)$$

where

$K_p = w_{rp}\,N\,A_p\,R_p/p$

= pump flow rate coefficient,

$C_t = C_{lp} + C_{lm}$

= Total leakage coefficient of the pump and motor.

3. State-Space Representation of the System

The next step is to develop the state space representation of the complete system. The state variables of the system can be defined as i, w_{sw}, q_{sw}, P_p and w_m.

Let us first begin with DC model and substitute Eq(2) into Eq.(1) and solve for $\dot{i}$ to yield

$$\dot{i} = -\frac{R}{L}\,i - \frac{K_b}{L}\,w_{sw} + \frac{E}{L} \qquad (26)$$

Also, substitution of Eq.(3) into Eq.(13) and solving for $\dot{w}_{sw}$ gives

$$\begin{aligned}\dot{w}_{sw} = {} & \frac{K_t}{(J_d + J_{sw})}\,i - \frac{(B_d + B_{sw})}{(J_d + J_{sw})}\,w_{sw} \\ & - \frac{S_2}{(J_d + J_{sw})}\,q_{sw} - \frac{K_{p2}}{(J_d + J_{sw})}\,P_p\,q_{sw} \\ & - \frac{S_1}{(J_d + J_{sw})} + \frac{K_{p1}}{(J_d + J_{sw})}P_p \\ & - \frac{a_{sw}}{(J_d + J_{sw})}\,(T_{ds} + T_{dc} + T_{swc})\end{aligned} \quad ... (27)$$

and one can easily remember that

$$\dot{q}_{sw} = w_{sw} \quad ..(28)$$

From Eq.(25), one can deduce the following equation

$$\dot{P}_p = -\frac{b_e C_{tm}}{V_t} P_p - \frac{b_e D_m}{V_t} w_m + \frac{b_e K_p}{V_t} \tan(q_{sw}) \quad ..(29)$$

The last state equation for $\dot{w}_m$ can be easily obtained from Eq.(23),

$$\dot{w}_m = \frac{D_m}{J_m} P_p - \frac{B_m}{J_m} w_m - \frac{a_m}{J_m} T_{mc} - \frac{1}{J_m} T_L \quad ..(30)$$

Based on Eqs.(26) to (30), the state equations of the complete system can be written in vector-matrix form:

$$\dot{\boldsymbol{x}} = \boldsymbol{A}\ \boldsymbol{x} + \boldsymbol{B}\ u_d + \boldsymbol{B_T}\ u_T \quad ..(31)$$

where

$\boldsymbol{x}$ is a state vector of the following variables:

$$\boldsymbol{x} = [i \quad w_{sw} \quad q_{sw} \quad P_p \quad w_m]$$

$\boldsymbol{A}$ is the state matrix and is given by

$$\boldsymbol{A} = \begin{bmatrix} a_{11} & a_{12} & a_{13} & a_{14} & a_{15} \\ a_{21} & a_{22} & a_{23} & a_{24} & a_{25} \\ a_{31} & a_{31} & a_{32} & a_{34} & a_{35} \\ a_{41} & a_{42} & a_{43} & a_{44} & a_{45} \\ a_{51} & a_{52} & a_{53} & a_{54} & a_{55} \end{bmatrix}$$

where

$a_{11} = -R/L$, $a_{12} = -K_b/L$

$a_{13} = a_{14} = a_{15} = 0$,

$a_{21} = K_t/(J_d + J_{sw})$,

$a_{23} = -S_2/(J_d + J_{sw})$,

$a_{22} = -(B_d + B_{sw})/(J_d + J_{sw})$,

$a_{25} = 0$, $a_{51} = a_{52} = a_{53} = 0$,

$a_{24} = (K_{p1} - K_{p2}\, x_3)/(J_d + J_{sw})$,

$a_{32} = 1$, $a_{31} = a_{33} = a_{34} = a_{35} = 0$,

$a_{44} = -b_e C_{tm}/V_t$, $a_{45} = -b_e D_m/V_t$,

$a_{42} = -b_e C_{tm}/V_t$, $a_{42} = a_{43} = 0$,

$a_{54} = D_m/J_m$ and $a_{55} = -B_m/J_m$

$\boldsymbol{B}$ is the input vector $[1/L \quad 0]^T$,

$\boldsymbol{u}$ is the input of the dc-motor E,

$\boldsymbol{B_T}$ is the input matrix due to torque and is given by

$$\boldsymbol{B_T} = \begin{bmatrix} 0 & 0 \\ a/J_d & 1/J_d \end{bmatrix},$$

$\boldsymbol{u_T}$ is the torque vector of the form

$$\boldsymbol{u_T} = [(T_{ds} + T_{dc}) \quad T_{sw}]^T .$$

4. Simulated Results

4.1. Open-loop Characteristics

Figure (6) shows the Simulink/s-function modeling of the open-loop hydraulic system.

The state space representation developed in Eq.(31) has peen coded in an m-file s-function type referred as “HydraulicSystem”. This file is listed in Appendix II. An s-function block from the Simulink library is required to be pulled down in a model file with the same name as the s-function m-file. For Simulink to recognize an m-file s-function, one must provide it with specific information about s-function. This information includes the number of inputs, outputs, states and other block characteristics [9].

During simulation of the model, Simulink repeatedly invokes the file “HydraulicSystem” using the flag argument to indicate the task to be performed. A continuous state-space with five states (DC-motor current, swashplate speed, swashplate angular position, pump pressure, and hydraulic motor speed) is assigned for this simulation. Therefore, flag 1 is used to indicate this task. The output

vector is returned through flag 3 and has the same size and variables as the state vector.

In Figure (7), the step input of height 10 v. is applied to the DC-motor without applying external hydraulic motor load. It is clear from Fig.(7-a) that DC motor current settles at 2 A one second later. One can see that the speed response of the swashplate, Fig.(7-b), suffers chattering at the beginning of simulation and then falls down to zero as soon as the swash plate angle reaches the saturated value 15 deg. One can also see the monotonic and well behaviors of motor speed, swashplate and pressure. It is worth to note that the dynamic responses of the motor speed and pump pressure follow the same envelope as that of swashplate angle. This is fairly justified, since the flow rate of hydraulic fluid is directly proportional the swashplate angle and, consequently, the motor speed and pressure is strongly related to swash angle changes. However, the pressure response shows a peak overshoot near the settling time, as it is shown in Fig.(7.e).

In Figure (8), the above procedure is repeated with the applied external hydraulic motor load. The load characteristic is described in Fig.(9). A 5-N.m load is suddenly applied at time 2 second and then released at time 3 second. Also, a negative pulse load of height 5-N.m is applied during the period 6-7 seconds. One can easily see that this load exertion has only affected the responses of hydraulic motor speed and pressure, i.e, Fig.(8.c) and Fig.(8.e). It is evident from the spikes of these responses at time of load exertion how the load changes degrade hydraulic motor responses. On the other hand, the DC current, Fig.(8-a), remained constant during load changes, as there is no feedback signal to feel the DC motor with these changes. Conseq- uently, the swashplate angular position, directly linked to DC motor, would never change as well. This is evident in Fig.(8-b), Fig.(8-d) and Fig.(8-e).

4.2. Closed-loop Characteristics

In the speed-controlled hydraulic system, two loops can be used for controlling the overall system. The inner loop is responsible for controlling the swashplate movement and the outer loop is required for speed control of hydraulic motor. It is advantageous to add a controller for each loop and to see the enhancements of these controllers to the corresponding responses.

Figure (10) shows the feedback connection of the inner loop; as the swashplate angle is fedback through a PI controller.

Figures (12), (13) and (14) shows the various responses of Fig.(10) to step input with different controller settings. Though the settling time of all response has much decreased (enhanced) as compared to those responses without inner loop, yet there are still problems. One can easily see the adverse effect of the inner loop on the dynamic responses of hydraulic motor speed and pressure. The inner loop causes an the oscillatory behavior in these

responses as shown Fig.(12-c), (13-c) and (14-c), and Fig.(12-e), (13-e) and (14-e)). Meanwhile a perfect response of swashplate angles has been obtained in Fig.s (12-d), (13-d) and (14-d). Also, one can see from the figures that increasing controller proportional gain (Kp) could lead to more oscillatory responses of hydraulic motor speed and pressure and the increased value of the integral gain (KI) make the DC motor draw high current, as it is illustrated in Fig.s(12-a), (13-a) and (14-a). The current of DC motor increases without bounds, Fig. (12-a) and (14-a), as integral term of the PI controller is included. This is due to the saturation of the swashplate and, then, the output signal from swashplate speed measuring unit is also saturated and no additional speed signal will be summed with the inner summer to give negative error or correction to the DC motor. Actually, in practice, this current is limited to the capability of the DC motor drive circuit.

Figure (11) shows the closed-loop system with inclusion of the outer loop. The speed controller is placed to monitor and control the speed error.

Figure (15) shows the various responses with the following controller setting values: Kp=0.1, KI=1 and Kd=0. Compared to responses without outer loop, there is a great improvement especially in the dynamic performances of hydraulic motor speed and pressure. However, a large noise and chattering has been observed in all responses of Fig.(15), but this noise is of significant in swashplate speed response Fig.(15-b). Practically, this chatter is expected to be a source of temperature rise.

Keeping the previous settings of speed controller, a positive and negative pulses of torque load, with the same characteristics of Fig.(9), are applied to the hydraulic motor shaft. The changes in behaviors of all variables are shown in Fig.(16). It is clear from the figure that the outer feedback caused the load changes to appear in the dynamic of the swashplate angle. Actually, the dips due to the load changes are much reduced as one retunes the terms of the speed controller.

It is instructive to see the effect of changing the rotational speed of the pump on the dynamic performance of different states. The value of speed has been increased to 250 rad/sec. The effect of this parameter is evident in the increased fluctuations in all responses at steady-state value. The responses with this change of parameter are shown in Fig.(17).

The value of bulk modulus of the fluid has been changed from 1.45 to 5. The fluctuations would increase especially in the swashplate speed dynamic response as demonstrated in Fig.(18). This increased frequency of fluctuations is justified as the spring property of the oil has been increased. Also, it is worth to note that the retuning the value of the speed controller terms has negligible effect on both the frequency and capacity of the fluctuations.

5. Conclusions

The addition of the inner loop would promote the dynamic behavior of the system responses;

yet, no chance for load changes to be seen on DC motor current, and then, on the swashplate dynamic behavior. Therefore, rejection of load changes is not possible with inner loop only.

The addition of the outer loop shows an oscillatory behavior to responses of hydraulic motor speed and pressures. However, this outer loop much enhances the settling time of overall speed-controlled system. Moreover, the addition of the outer loop would reflect the load changes on the hydraulic motor shaft on the various system responses.

The increased value of integral action of the PI controller would lead the DC motor current to increase without bound. However, this study presents a theoretical analysis, since the DC motor current is practically limited by its drive circuit.

Increasing bulk of modulus would increase the spring property of the fluid and this could increase the frequency of fluctuations that appear in the system responses.

As the results showed and from control point of view, the system performance degrades as varying the system parameters. Unfortu nately, the PID controller lacks the ability to on-line compensate such parameter variations, unless the controller terms are repeatedly retuned. Therefore, one can conclude that the PID controller is not intelligent against variations of system parameters and, hence, that requires other adaptive or intelligent technique to overcome the problem. Another way to enhance the performance of the conventional controller is linearize the model around specific operating point. However, the PID might again fail due time-varying nature of most hydraulic systems.

As shown earlier, the composite hydraulic system is of nonlinear nature. This is due the product of some states and the saturated characteristics of others. In fact, the presence of such nonlinearity accounts for PID controller failure against parameter variations.

The results showed that the inner loop controller could significantly improve the dynamic performance of the swashplate, while the outer loop has enhanced the responses of both hydraulic motor speed and pressure.

Modeling the studied hydraulic system in Simulink/s-function is similar to create a built-in continuous state-space block of the system. This s-function modeling can be used as starting point for a block that models the studied hydraulic system with time-varying coefficients.

The proposed control config-uration suggests eliminating of the bypass valve and to permit the swashplate of the variable displacement pump to swing in both directions. This, of course, would lead to bi-directional pump flow, which, in turn, controls the direction of hydraulic motor motion.

References

[1] Tonglin Shang "**Improving Performance of Energy Efficient Hydraulic Circuit**", Thesis, University of Saskatchewan, April 2004.

[2] Noah D. Manring, Fikreadam A. Damtew "**The Control Torque on the Swash Plate of an Axial-Piston Pump Utilizing Piston-Bore Springs**", Journal of Dynamic Systems, Measurement and Control, 2001, Vol. 123.

[3] Ali Volkan Akkaya, "**Effect of Bulk Modulus on Performance of a Hydrostatic transmission Control System**", Sadhana Vol. 31, Part 5, pp. 543-556, October 2006.

[4] Benjamin C. Kuo, Farid Golnaraghi, **"Automatic Control Systems"**, John Wiley & Sons, Inc., 2006.

[5] G. J. Schoenau, R. T. Burton, G. P Kavanagh, **"Dynamic Analysis of a Variable Displacement Pump"**, Journal of Dynamic Systems, Measurement and Control, 1990, Vol. 112.

[6] Ravi Doddannavar, Andries Barnard, "**Practical Hydraulic System"**, Elsevier Science & Technology Books, March 2005.

[7] Merritt, H., 1967, "**Hydraulic Control Systems"**, John Wiley & Sons, Inc., New York.

[8] Math Works, Inc., **"SIMULINK user's Guide**," Version 2, Jan 1997.

[9] **"Short Tutorial on Matlab,"** Tomas Co., 2004.

Appendix I

The following table is a list of all constants, coefficients and parameters of the hydraulic motor, DC motor and hydraulic pump used in the study [1].

Table (1) System parameters

Hydraulic Motor	Volumetric displacement of the motor D_m	2.38×10^{-6} m^3/rad
	Inertia of the motor and the load J_m	0.0016 $N\cdot m.\ s^2/rad$
	Motor leakage coefficient C_{tm}	2×10^{-13} $m^3/s\cdot rad$
	Motor damping ratio B_m	0.044 $N\cdot m.\ s/rad$
	Motor coulomb friction torque T_{fm}	2.14 $N\cdot m$
	Volume of the motor and pipe V_m	2.4×10^{-4} m^3
DC Motor	Terminal resistance R	4.83 Ω
	Terminal inductance L	0.0332 H
	Torque sensitivity K_t	2.27 $N\cdot m./A$
	Back EMF constant K_b	2.27 $V.\ s/rad$
	Moment of Inertia of the motor rotor J_d	1.4×10^{-3} $N\cdot m.\cdot s^2/rad$
	Viscosity damping coefficient B_d	1.43 $N\cdot m.\ s/rad$
Hydraulic Pump	Pump rotational speed	183.3 rad/s
	Number of pistons N	9
	Piston area A_p	83.5×10^{-4} m^2
	Viscous damping ratio of the swash plate B_{sw}	0.28 $N\cdot m\cdot s/rad$
	Piston pitch radius R_p	0.0224 m
	Maximum pump displacement D_p	1.95×10^{-6} m^3/rad
	Bulk modulus of the fluid b_e	1.45×10^{9} Pa
	Total pump leakage flow coefficient C_{tp}	4.3×10^{-13} $m^3\ Pa/s$

Volume of pump V_p (high pressure side)	$3\times10^{-5}\ m^3$
Average swashplate yoke inertia J_{sw}	$1.06\times10^{-3}\ N\cdot m.\ s^2/rad$

Appendix II
Hydraulic system S-function-Type m-File Listing

```
function [sys,x0,str,ts]
=HydraulicSystem(t,x,u,flag)
global R L Kt Kb Jd Bd Bsw Tds Tdc Tswc
Tmc Jsw  Kp1 Kp2 S1 S2;
global wre N Ap Rp Kp Be Vp Vm Vt Ct Dm
Jm Bm;
global x1 x2 x3 x4 x5;
if flag==0,
R=4.83;       % Terminal resistance
L=0.0332;     % Terminal inductance
Kt=2.27;      % Torque sensitivity
Kb=2.27;      % Back EMF constant
Jd=1.4e-3;    % Moment of inertia of the
               % motor rotor
Bd=1.43e-3;   % Viscous damping coefficient
Bsw=0.28;     % Viscous damping ratio of the
               % swash plate
Tds=0;        % Static friction torque
Tdc=0;        % Coloumb friction torque
Tswc=0.36;    % Coulomb friction torque of
               % the pump
Tmc=2.14      % Motor coulomb fiction torque
Jsw=1.06e-3;  % Average swashplate yoke
               % inertia
Kp1=7.46e-7;  % Pressure torque constant
Kp2=8.3e-7;   % Pressure torque constant
S1=0.096;  % Simplified pump model constant
S2=2.36;   % Simplified pump model constant
wre=183.3  % Pump rotational speed
N=9           % Number of pistons
Ap=83.5e-6  % Piston area
Rp=0.0224   % Piston pitch radius
Kp=wre*N*Ap*Rp/pi   % Pump flow rate
                     % coefficient
Be=1.45e9;      % Bulk modulus of the fluid
Vp=3e-5 ;       % Volume of pump (high
                % pressure side)
Vm=2.4e-4       % Volume of the motor and
                % pipe
Vt=Vp+Vm;       % Total volume (Pump and
                % Motor)
Clm=2e-13       % Motor leakage coefficient
Clp=4.3e-13;    % Pump leakage coefficient
Ct=Clp+Clm      % Total leakage coefficient of
                % the Pump
                % and motor
Dm=2.38e-6      % Volumetric displacement
                % of the motor
Jm=0.0016       % Inertia of the motor and
                % load
Bm=0.044        % Motor damping ratio
x0=[0,0,0,0,0];  % zero initial condition
x1=0;x2=0;x3=0; % Dummy variables
x4=0;x5=0       %
ts=[0 0];       %Initialize the array of
sample times
str=[];
sys=[5,0,5,2,0,0,1];  % 5 constinuos state, no
                      % discrete
 % states, 5 outputs 1 inputs, no of
 % directfeedthrough, one sample time
elseif flag==1,
E=u(1);TL=u(2);x1=x(1);x2=x(2);x3=x(3);
x4=x(4);x5=x(5);asw=sign(x2);am=sign(x5);
Tsc=Tdc+Tds+Tswc+Tmc;
a11=-R/L;a12=-Kb/L;a13=0;a14=0;a15=0;
a21=Kt/(Jd+Jsw);a22=-(Bd+Bsw)/(Jd+Jsw);
a23=-S2/(Jd+Jsw);a24=(Kp1-
Kp2*x3)/(Jd+Jsw);a25=0;
a31=0;a32=1;a33=0;a34=0;a35=0;
a41=0;a42=0;a43=Be*Kp/Vt;a44=-
Be*Ct/Vt;a45=-Be*Dm/Vt;
a51=0;a52=0;a53=0;a53=0;a54=Dm/Jm;
a55=-Bm/Jm;
if (x3>=0.2618) & (x1>0), % 15*pi/180
x(2)=0; a21=0; a22=0;a23=0; a24=0;
x3=0.2618 x2=0;
 elseif (x3<=-0.2618) & (x1<0),
x(2)=0; a21=0;a22=0; a23=0; a24=0; x3=-
0.2618;x2=0;
 end;
A=[a11, a12, a13, a14, a15
    a21, a23, a23, a24, a25
    a31, a32, a33, a34, a35
    a41, a42, a43, a44, a45
    a51, a52, a53, a54, a55];
Bi=[1/L;0;0;0;0];
BT=[0;-(asw+am)/(Jd+Jsw);0;0;0];
Bs=[0;-1/(Jd+Jsw);0;0;0];
BL=[0;0;0;0;-1/Jm];
sys=A*x+Bi*E+BT*Tsc+Bs*S1+BL*TL;
elseif flag==3,
   sys=[x1,x2,x3,x4,x5];
else
   sys=[];
end;
```

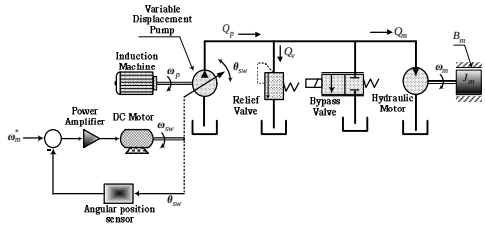

Figure (1) Speed Control of Pump-controlled system with bypass flow valve control

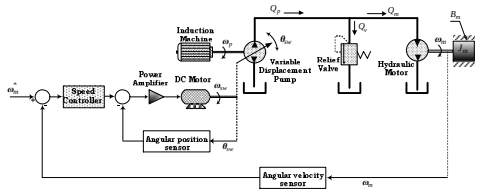

Figure (2) Speed control hydraulic system with reversal pump flow and reversal motor motion

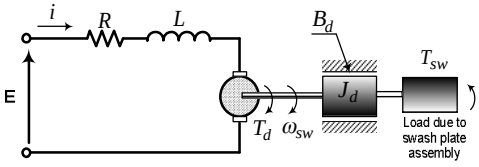

Figure (3) Schematic diagram of a DC motor

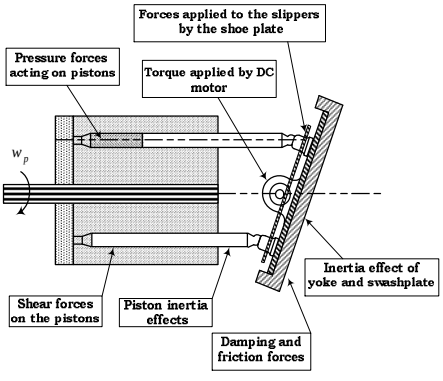

Figure (4) Forces which cause torques acting on the swashplate and yoke assembly.

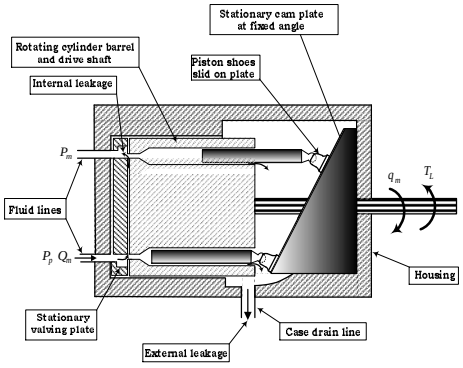

Figure (5) Schematic diagram of a fixed displacement axial piston motor [7]

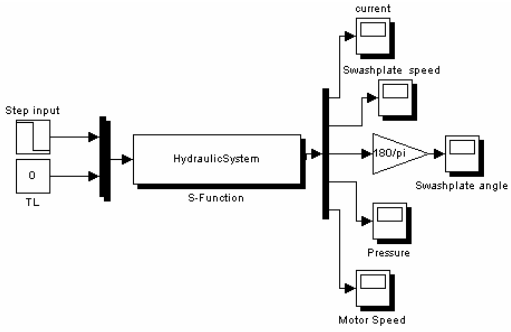

Figure (6) Simulink/s-function model of open-loop hydraulic system

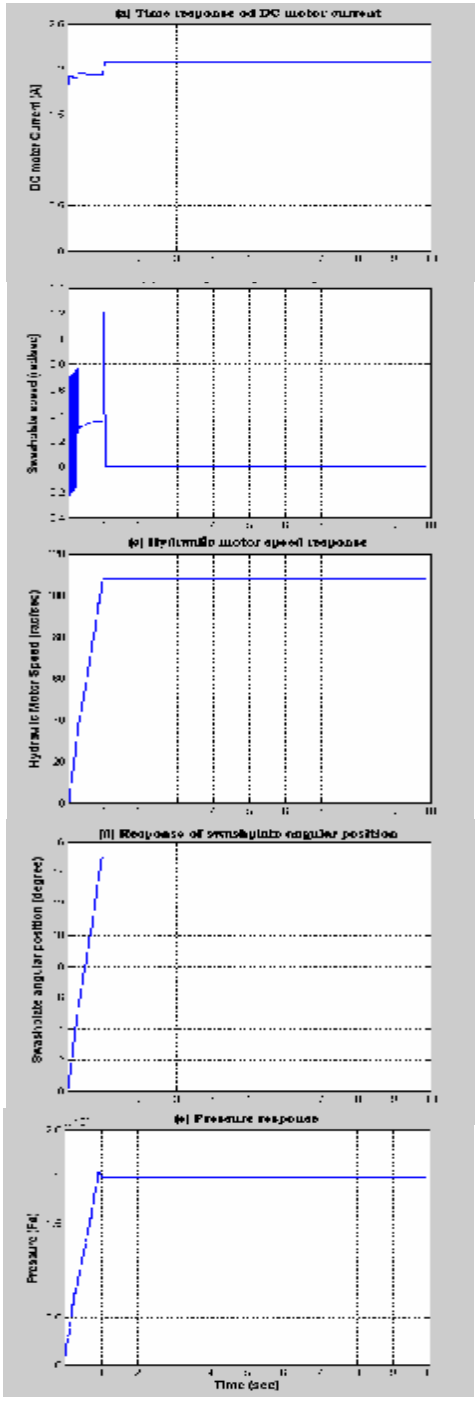

Figure (7) Open–loop test with step input

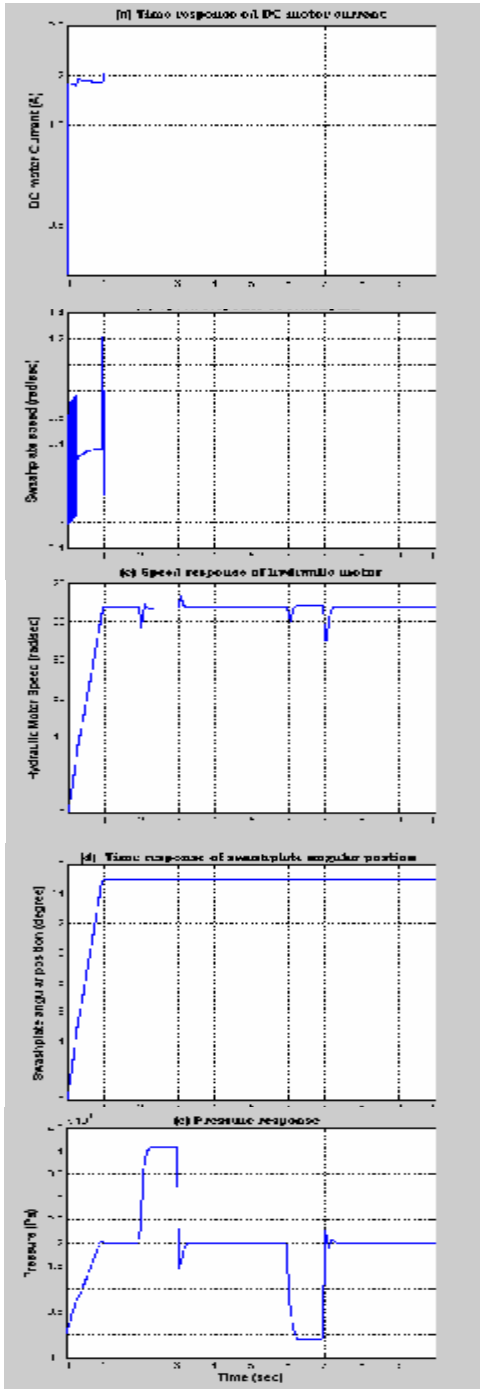

Figure (8) Open–loop test with step input and applied sudden motor load change

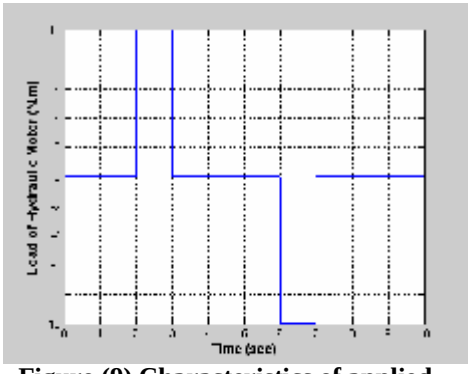

Figure (9) Characteristics of applied motor load

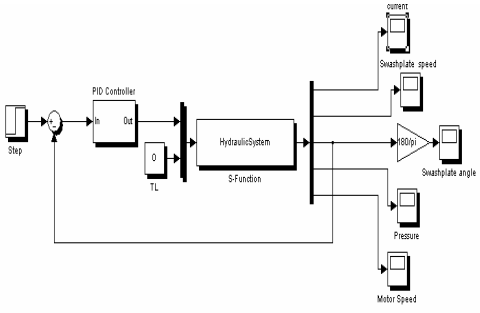

Figure (10) Simulink/s-function model of hydraulic system with inclusion of angle feedback signal

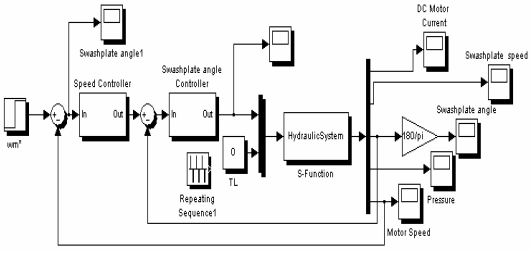

Figure (11) Simulink/s-function model of closed-loop hydraulic system (inclusion of speed and angle signals of swashplate)

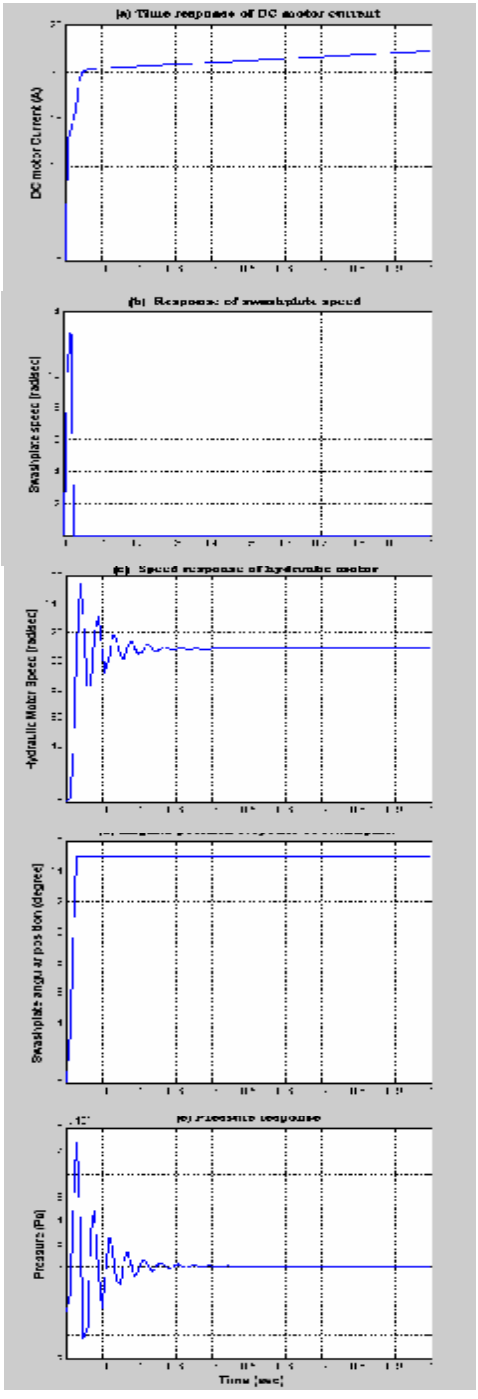

Figure (12) Hydraulic system responses with only inner loop and controller gains KI=1, Kp=10

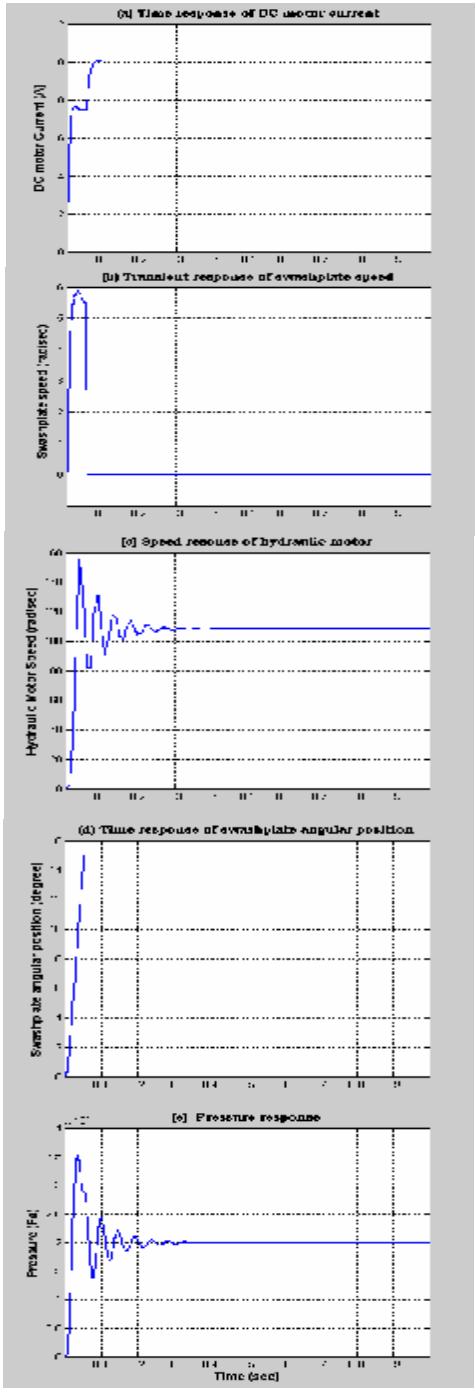

Figure (13) Hydraulic system responses with only inner loop and controller gains KI=0, Kp=5

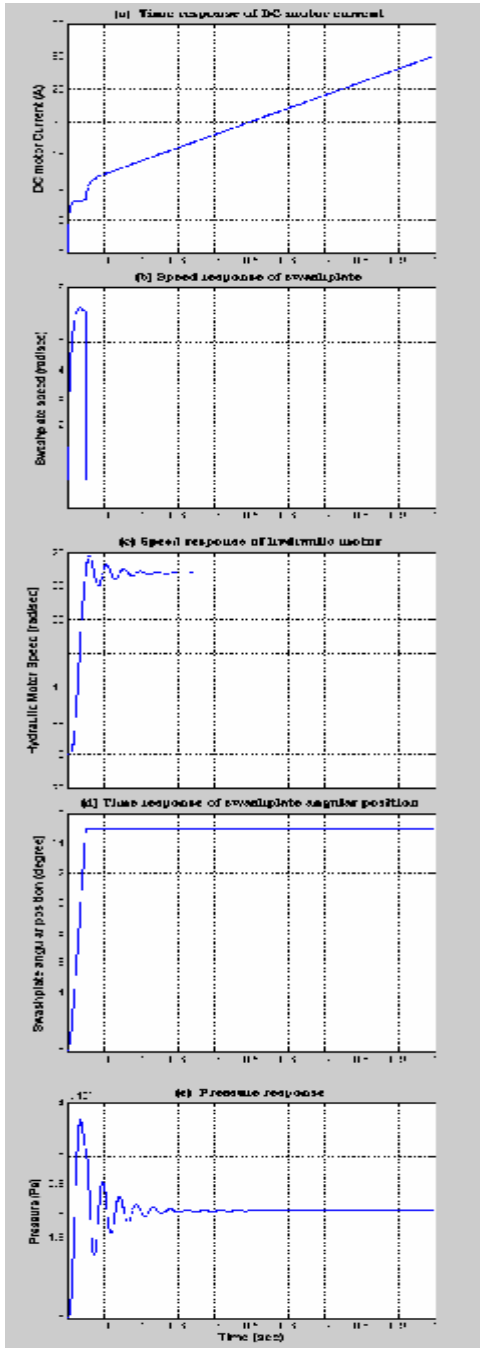

Figure (14) Closed -loop hydraulic system with only inner loop and controller gains KI=10, Kp=5

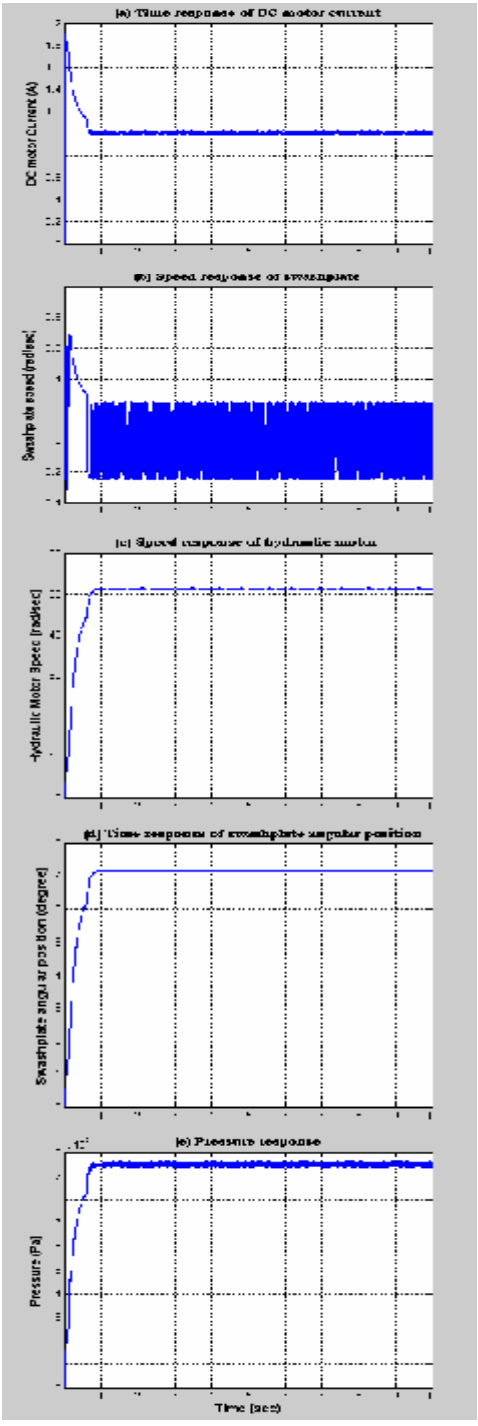

Figure (15) Closed -loop hydraulic system with both loops

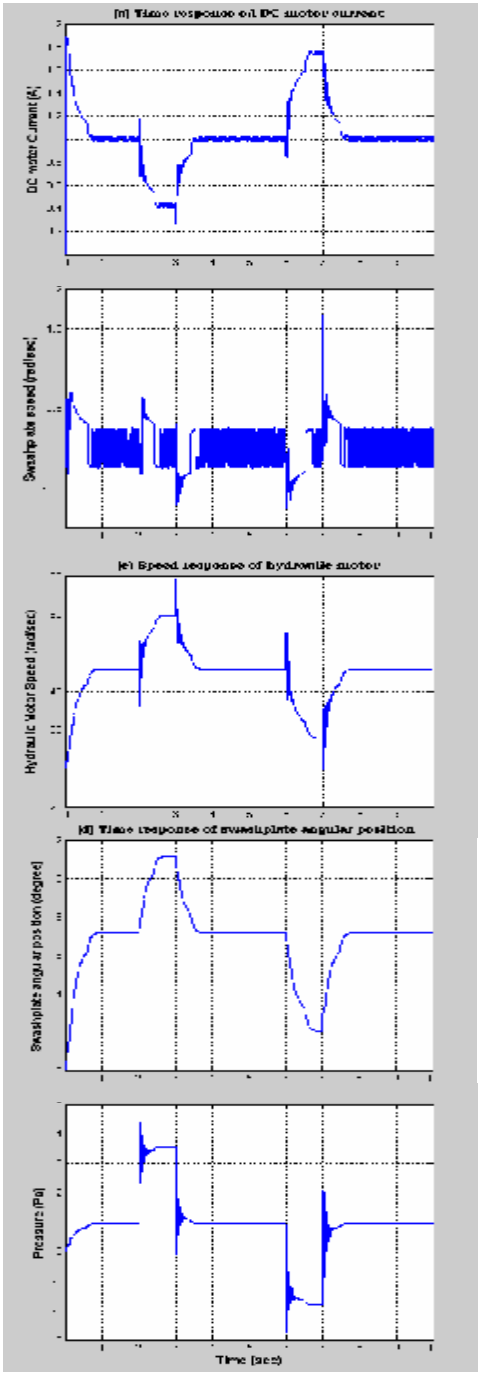

Figure (16) Closed -loop hydraulic system with both loops and cyclic load changes

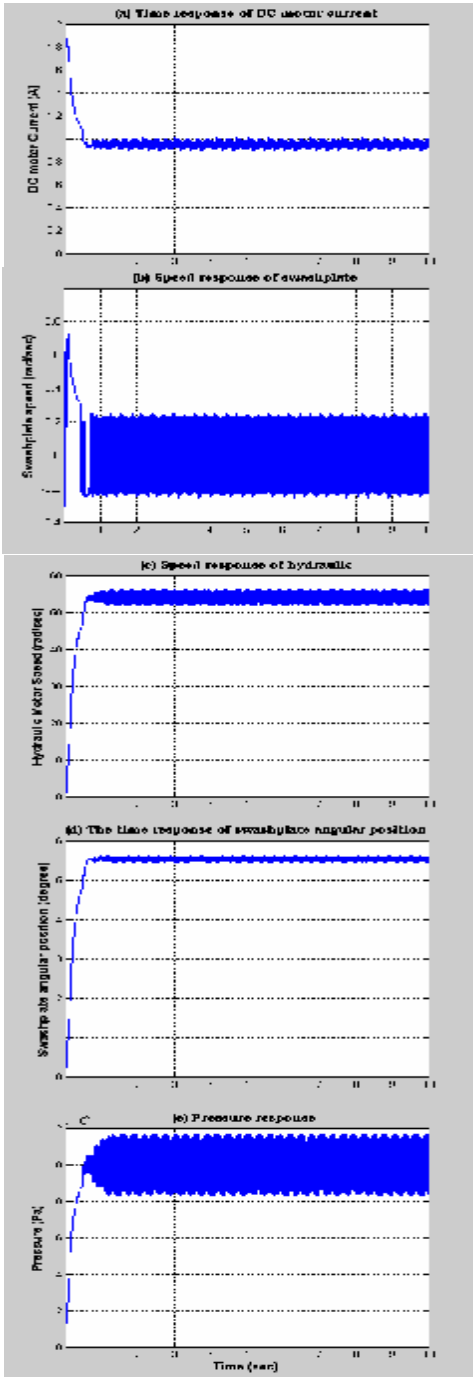

Figure (17) Closed -loop hydraulic system with both loops and another pump speed

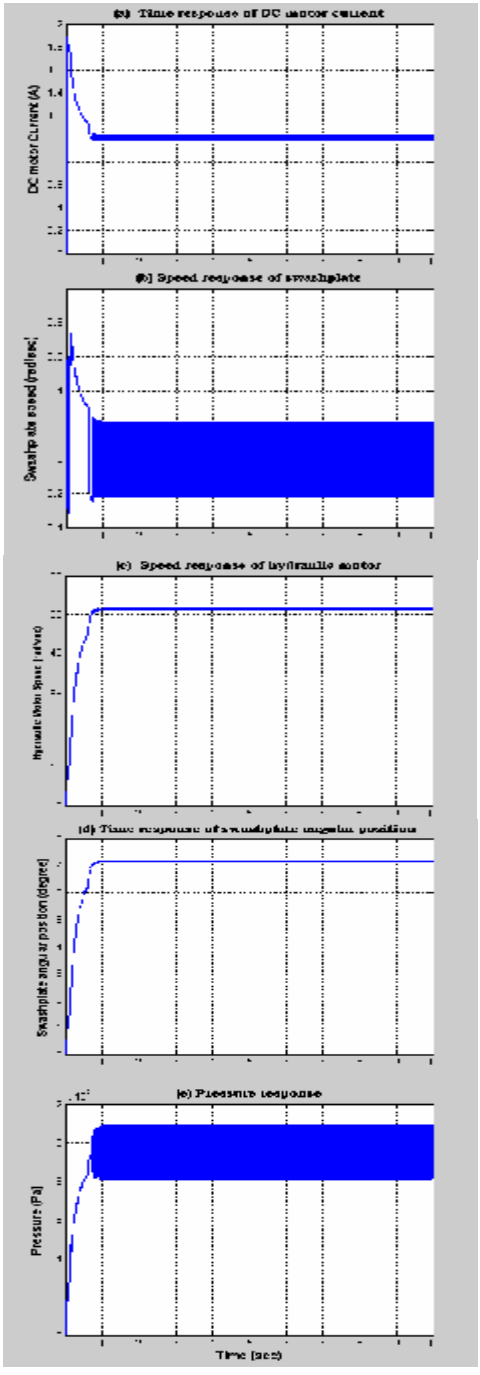

Figure (18) Closed -loop hydraulic system with both loops and another value of Bulk modulus